

# Modification of Hadron Properties in Dense Nuclear Matter

---

**Victoria Zinyuk\* for the FOPI Collaboration †**

*Physikalisches Institut der Universitat Heidelberg, Heidelberg, Germany*

*E-mail: [V.Zinyuk@gsi.de](mailto:V.Zinyuk@gsi.de)*

Strange particles produced sub- or close-to-production threshold allow to probe the properties of hot and dense baryonic matter. Hadron properties like cross sections, width and effective mass are believed to alter under these conditions and influence the production and propagation of hadrons in nuclear medium. In this review we report on the flow observables for p,  $K^+$ - and  $K^-$  mesons in  $^{58}\text{Ni}+^{58}\text{Ni}$  collisions and on the phase space population of  $K^+$ - and  $K^-$  mesons in pion induced reactions.

*International Winter Meeting on Nuclear Physics,  
27-31 January 2014  
Bormio, Italy*

---

\*Speaker.

†Supported by BMBF 05P12VHFC7

## 1. Introduction

Baryonic matter created in nucleus-nucleus collisions in SIS18 energy regime is compressed to about 2-3 times the normal nuclear matter density ( $\rho_0$ ) and heated up to temperatures around 100 MeV [1][2]. Under these conditions several non-trivial in-medium effects such as partial restoration of chiral symmetry, modification of meson-baryon coupling and nucleon potentials are predicted. As a result the properties of hadrons in nuclear medium change compared to hadrons in vacuum. Expected modification of production cross sections, width or mass may influence the experimentally accessible phase space distribution of hadrons in the final state.

Strange particles, like K mesons, probe the dense phase of the collision. In a mean-field approach the influence from the medium can be parametrized as a density dependent mean field  $KN(\bar{K}N)$ -potential, repelling(attracting) the kaons(anti-kaons) toward nucleons [3].

The FOPI spectrometer (described elsewhere [4]), located at GSI, Darmstadt allows the identification of charged particle within nearly full azimuthal acceptance and a large span of longitudinal angle. Charged kaons can be identified in the momentum range  $0.1 \text{ GeV}/c < p_{LAB} < 1 \text{ GeV}/c$ . This low momentum region is considered to be highly sensitive to possible in-medium modifications.

In the following we discuss two observables for  $K^+$  and  $K^-$  mesons: The collective flow [5] in Ni+Ni at 1.9 AGeV and ‘momentum ratios’ in pion-induced reactions.

## 2. Azimuthal Anisotropies

The attraction/repulsion of kaons by nucleons influence their propagation through the nuclear medium. If the nucleons have a preferential propagation direction(e.g. due to density gradient) the azimuthal distribution of kaons are affected, resulting in anisotropies of the azimuthal distribution in the final state.

Anisotropies in the azimuthal emission pattern can be quantified by expressing the azimuthal distribution in a Fourier series:

$$\frac{dN}{d\phi} \propto (1 + 2v_1 \cos(\phi) + 2v_2 \cos(2\phi) + \dots), \quad (2.1)$$

with  $\phi$  the azimuthal angle of the outgoing particle with respect to the reaction plane [6]. The reaction plane is reconstructed event-wise by the transverse momentum method [7]. The Fourier coefficients are corrected for the accuracy of the reaction plane determination (eventwise) according to the Ollitrault method [8] (for values see Tab. 1). For the details of the experimental analysis see [9].

The first order Fourier coefficient,  $v_1$ , describes the collective sideward deflection of particles in- (reaction) plane, called ‘directed flow’. In the upper panels of Fig. 1  $v_1$  is shown as a function of normalized rapidity  $y_{(0)} = y_{lab}/y_{cm} - 1$  for three different particles. The centrality of the evaluated reactions is summarized in Tab. 1. The particles shown in Fig. 1 originate from the sample (a). (For more details see [9]). At mid-rapidity ( $y_{(0)} = 0$ ) by construction  $v_1=0$ , i.e. the emission is isotropic. Toward the target rapidity ( $y_{(0)} = 1$ ) protons propagate collectively in a preferential direction, i.e. the value of  $v_1$  becomes negative.  $K^+$  mesons (middle panel) are collectively deflected in-plane in

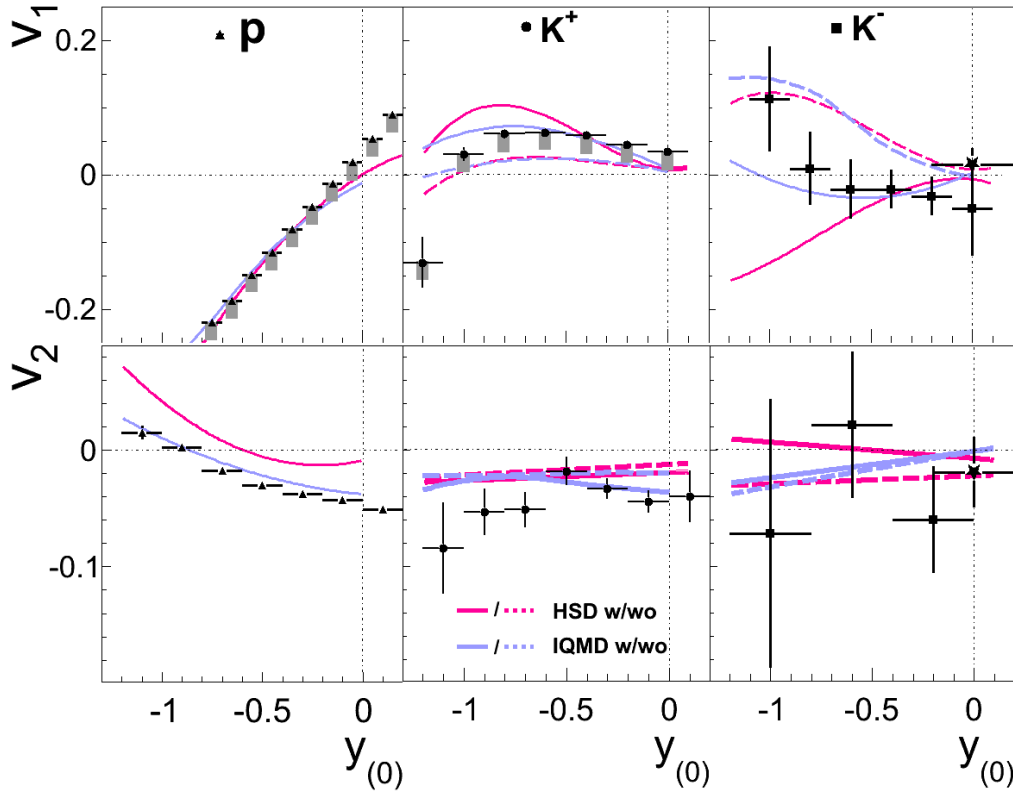


**Figure 1:** First and second Fourier Coefficients  $v_1$  and  $v_2$  as a function of normalized rapidity for protons (right panels),  $K^+$  mesons (middle panels) and  $K^-$  mesons (left panels) compared to the prediction of HSD (red) and IQMD (blue) transport models with (solid lines) and without (dashed lines) the assumption of KN-potential. Error bars (boxes) denote the statistical (systematic) uncertainties. Note: Model calculations without in-medium potential (dashed lines) still include  $K^+N$  ( $K^-N$ ) rescattering and absorption processes for  $K^-$ . [9]

the direction opposed to that of protons. This behavior is consistent with the idea of repulsion of  $K^+$  mesons from protons.

The second order Fourier coefficient,  $v_2$ , describes the emission probability in - versus out - of the reaction plane, referred to as ‘elliptic flow’ [10, 11]. Protons and  $K^+$  mesons are observed to collectively move out-of-plane at mid-rapidity (Fig. 1 lower panel) as indicated by the negative  $v_2$  values. For protons the absolute value of  $v_2$  diminishes as the in-plane contribution gets larger toward the target rapidity.

For  $K^-$  mesons (Fig. 1 right panel) the values of  $v_1$  and  $v_2$  are compatible with zero within the statistical uncertainties for all rapidities, i.e. the  $K^-$ 's are emitted isotropically both in- and out-of plane. The conclusions on a possible attractive potential of  $K^-$  are difficult.  $K^-$  mesons, at considered momenta, have a small mean free path in nuclear matter and therefore are expected to suffer scattering and absorption. Especially the absorptive processes have a strong influence on the azimuthal patterns in the final state.

To evaluate the data with regard to the depth of the  $KN(\bar{K}N)$ -potential we compare our experimental findings to transport model predictions with and without the assumption of an additional

	Mul	$\sigma$ [b]	$\langle b \rangle \pm \Delta b$ [fm]	$f_1$	$f_2$
(a)	[20, 90]	$1.09 \pm 0.1$	$3.90 \pm 1.41$	$1.5 \pm 0.1$	$3.0 \pm 0.1$
(p)	[20, 48]	$0.79 \pm 0.05$	$4.54 \pm 0.95$	$1.5 \pm 0.1$	$3.0 \pm 0.1$
(c)	[49, 90]	$0.3 \pm 0.05$	$2.11 \pm 0.80$	$1.6 \pm 0.1$	$3.1 \pm 0.2$

**Table 1:** Definition of event classes: (a) total, (p) peripheral and (c) central events. The baryon multiplicity Mul contains all charged particles from the Plastic Wall ( $6.5^\circ < \theta_{lab} < 23^\circ$ ) and p, d, t,  $^3He$  and  $\alpha$  from the CDC. The corresponding cross section  $\sigma$ , mean impact parameter  $\langle b \rangle$ , the RMS of  $\langle b \rangle$ :  $\Delta b$  and the reaction plane correction factors  $f_1$  for  $v_1$  and  $f_2$  for  $v_2$  are listed. Centrality selection, imposed on the data, is realized by weighting the events with an impact parameter dependent function, that is obtained by evaluating the influence of the multiplicity selection on the impact parameter distribution within the IQMD model [13] that describes the multiplicity distribution reasonably well.

attractive/repulsive interaction of antikaons/kaons with nuclear matter. The results of two different calculations are evaluated: The Hadron String Dynamics (HSD) model [12] and the Isospin Quantum Molecular Dynamics (IQMD) [13]. In both HSD and IQMD a  $KN$ -potential of  $20 \pm 5$  MeV for particles at rest ( $p = 0$ ), at normal nuclear matter density and a linear baryon density dependence is employed. A similar, but attractive potential is used in IQMD as  $K^-N$ -potential with  $U_{K^-N}(\rho = \rho_0, p = 0) = -45$  MeV (also referred to as ‘half potential’) and a G-Matrix formalism corresponding to  $U_{K^-N}(\rho = \rho_0, p = 0) = -50$  MeV is employed in HSD [14]. For details on both transport codes see [15]. In Fig. 1 the results of transport model predictions for in-medium modified propagation are show by the full lines and the flow patterns of free propagating particles are denoted by the dashed lines.

Note: For all HSD and IQMD prediction with and without in-medium modifications absorption and rescattering are taken into account by the transport calculations.

Transport models suggest that the repulsive  $K^+N$ -potential changes the emission patterns of  $K^+$  mesons from isotropic emission ( $v_1$  and  $v_2$  values are close to zero, dashed lines in Fig. 1 middle panel) to in-plane emission. The largest sensitivity is expected in the sideflow observable  $v_1$  at backward(near target) rapidities. This effect is observed in the experimental data and reproduced within in-medium modified IQMD prediction. The HSD calculation with  $K^+N$ -potential overpredicts the magnitude of ‘antiflow’.

For  $K^-$  meson the interpretation is different. Free propagating  $K^-$ ’s generate an ‘antiflow’ signature, which is attributed to the strong absorption by strangeness exchange reactions with baryons. The attractive  $K^-N$ -potential manifest itself in a ‘flow’ signature. HSD predicts  $v_1$  values similar to that of protons. IQMD also predict a ‘flow’ signature but with a slightly different rapidity dependence and smaller magnitude. The experimental data favors the IQMD calculation with the assumption of  $U_{K^-N}(\rho = \rho_0, p = 0) = -45$  MeV.

Even though the HSD and IQMD prediction of in-medium modified flow patterns are different, the prediction without in-medium modifications agree, therefore an attractive  $K^-N$ -potential is clearly necessary to explain the experimentally observed  $v_1$ -values.

The squeeze-out signature at midrapidity ( $v_2$ ) of  $K^+$  (Fig. 1) is describes within IQMD by a presence of a  $KN$ -potential. HSD prediction deviates from the data by  $\sim 2 \Delta v_1$ . (The evaluation of  $\Delta v_n$  can be found in [9]). In another rapidity regions and in case of  $K^-$  (Fig. 1) no conclusions

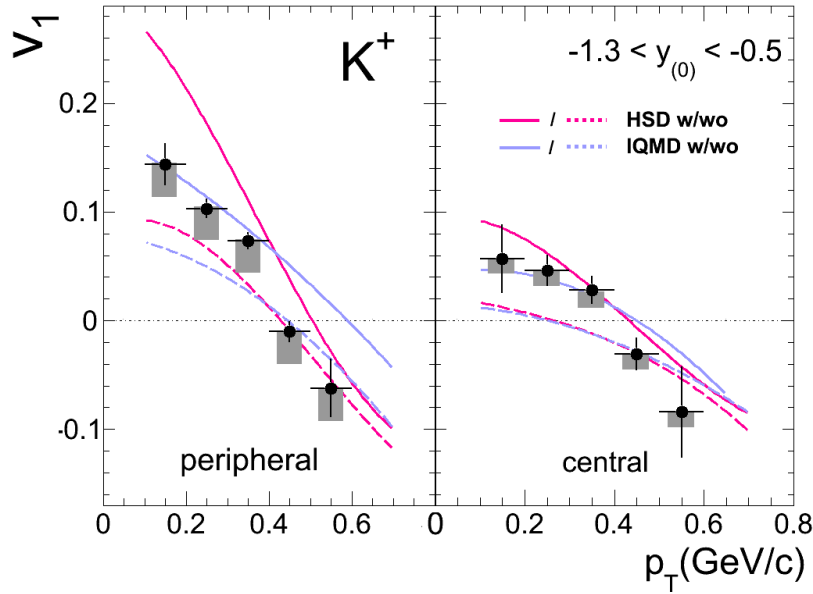


**Figure 2:** First Fourier Coefficient as a function of transverse momentum in the near-target rapidity for  $K^+$ -mesons *Left:* Peripheral event selection *Right:* Semi-central event selection (see Table 1) The data is compared to HSD (red) and IQMD (blue) transport approaches with (solid lines) and without (dashed lines) the assumption of a  $K^+N$ -potential. [9]

about the presence of an in-medium potential can be drawn from this observable with statistic sensitivity of the data.

The accumulated statistics for  $K^+$  allow to further investigate the discrepancy of transport predictions with the data shown in Fig. 1 by evaluating in Fig. 2 the dependence of  $v_1$  on the transverse momentum  $p_T$  near target rapidity ( $-1.3 < y_{(0)} < -0.5$ ) for the two centrality classes (p) and (c) defined in Table 1.

The data shows a strong  $p_T$  dependence, i.e. drop with increasing momentum. This is explained by the close-to threshold production of kaons. Near the production threshold beam energies, the major part of kaons is produced with small momenta. The kaons gain momentum by rescattering with energetic nucleons and therefore their flow strength increases in the direction of nucleons [16]. The  $v_1$  values of protons are negative (Fig. 1, left panel) and therefore the  $v_1$  values of  $K^+$  decrease with increasing momentum.

The  $p_T$  dependence in peripheral collisions is stronger than in central ones. This is attributed to the larger density gradient in peripheral collisions causing stronger in-plane deflection of kaons from peripheral compared to that from central events.

In the central event sample the data is described by the HSD calculation with  $U_{K+N} = 20$  MeV in agreement with the previous FOPI data [11]. In the peripheral event sample, HSD overestimates the magnitude of  $v_1$  especially at low  $p_T$ . IQMD reproduce the  $p_T$ -dependence of  $v_1$  in both centrality samples reasonably well.

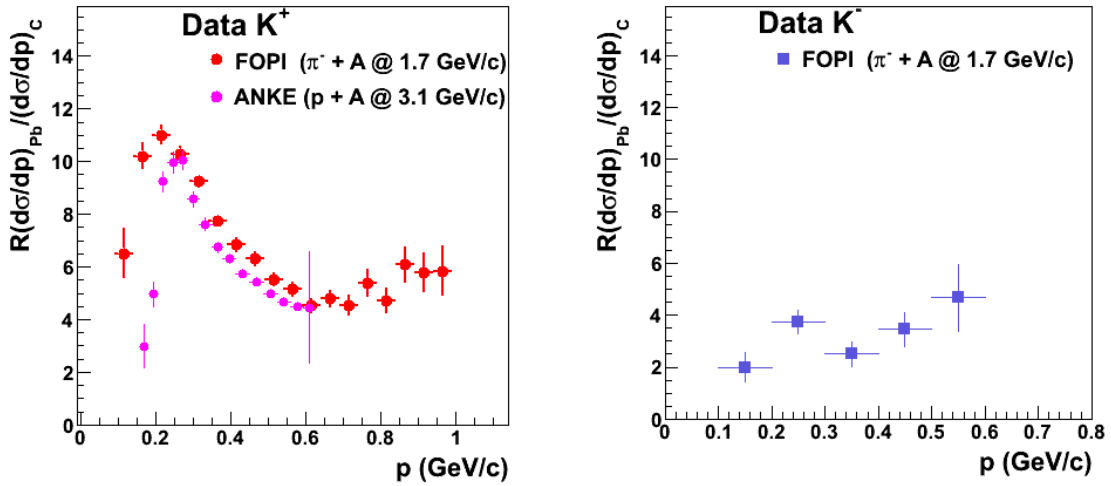


**Figure 3:** Ratio of momentum distributions of charged kaons produced in a heavy target to light target.

### 3. Ratio of Momentum Distributions

When a heavy target, like lead, is irradiated with a pion beam the first  $\pi + p/n$  collisions will happen at the surface of the lead nucleus. A strange particle (e.g. kaon) produced in that collision is influenced by the nucleons of the lead nucleus, i.e. nuclear matter at  $\rho = \rho_0$  and  $T = 0$ . At  $\rho = \rho_0$  and  $T = 0$  the value of the chiral condensate, responsible for the spontaneous breaking of chiral symmetry, is expected to drop by  $\sim 30\%$ . This and another in-medium effects can be studied at normal nuclear matter density in pion induced reactions.

The FOPI Collaboration in cooperation with the GEM-TPC Collaboration has measured  $\pi^- + {}^{208}\text{Pb}$ ,  $\pi^- + {}^{63}\text{Cu}$  and  $\pi^- + {}^{12}\text{C}$  collisions. The beam momentum was set to 1.7 GeV/c to make the direct production of  $K^+K^-$ -pairs possible. After background subtraction about 16000/19000 (produced in C/Pb-target)  $K^+$ - and about 450/230 (C/Pb-target)  $K^-$  candidates could be identified. Both  $K^+$ - and  $K^-$ -mesons could be measured in an almost full dynamic range, down to  $p_K = 0.1\text{ GeV}/c$  disclosing the most sensitive phase space region for  $KN(\bar{K}N)$ -potential investigation.

To see a possible influence from nuclear potentials we evaluate the momentum distributions of K-mesons. The momentum distribution of  $K^+$  mesons produced in Pb-target ( $(dN/dp)_{Pb}$ ) should be shifted to higher momenta with respect to the one of  $K^+$  mesons from the C-target ( $(dN/dp)_C$ ) if the  $K^+$  mesons are repelled by nuclear matter. (For detailed description of the observable see [17].) The ‘momentum ratio’  $R((d\sigma/dp)_{Pb}/(d\sigma/dp)_C)$ , normalized to the geometrical cross section, is shown in Fig. 3.

For  $K^+$ -mesons the repulsion from nucleons has two contributions. The first originates from the strong interaction and reflects the in-medium modification for kaons, the second repulsion is due to the Coulomb-interaction. The difference of these two contributions can be observed by comparing the ‘momentum ratios’ of  $K^0$  and  $K^+$  mesons - equal to the strong interaction, but carrying different electric charge. This comparison is done in [18]. In the repulsion scenario the momentum ratio is expected to undergo a maximum. Left panel of Fig. 3 shows the result for  $K^+$  mesons from the recent data sample. This measurement confirms the expected behavior and it is in qualitative agreement with the previous results by the FOPI Collaboration ( $K_S^0$  measurement [18])

and ANKE collaborations ( $K^+$  measurement [19]) showing a maximum around  $p_{K^+} = 0.25 \text{ GeV}/c$ . However we do not observe the strong decrease, as seen bei ANKE, at smaller momenta, possibly due to different intermediate states.

In the attraction scenario provided by  $\bar{K}N$ -potential the ‘momentum ratio’ would have the largest value at smallest momentum and decrease with increasing momenta. Fig. 3 (right panel) reveals that  $K^-$  mesons show a nearly constant ratio. A possible reason is the small mean free path (on the scale of both lead and carbon nuclei) and therefore the strong absorption in nuclear matter. Presumably the observed  $K^-$  mesons are emitted from the surface of the target nucleus, do not feel the  $\bar{K}N$ -potential within the nucleus, and therefore have the same phase space distribution in both targets. The beam momentum of  $1.7 \text{ GeV}/c$  allows the direct production of  $K^+K^-$ -pairs and hence also the production of intermediate  $\phi$  mesons decaying to  $K^+K^-$  (48.9 % BR). Currently it is not clear to which extent the observed  $K^-$  mesons originate from  $\phi$  meson decays.

#### 4. Conclusion

The sideflow observable  $v_1$  of kaons and antikaons produced close to the threshold energies shows sensitivity to the influence from the  $KN(\bar{K}N)$ -potential. Evidences for a repulsive  $KN$ -potential and a weakly attractive  $\bar{K}N$ -potential are found in comparison to transport model calculation.

Despite large effort from both theoretical and experimental side the description of kaons, especially of  $K^-$  in hot medium at  $\rho = 2-3 \rho_0$  is not comprehensive. A step toward a solution can be a simpler system of cold matter at normal nuclear matter density as created in pion induced reactions. The ratio of momentum distributions provide a stable observable not sensitive to the experimental efficiency and systematic uncertainties. However at energies above the production threshold for  $K^-$  meson the measurement is contaminated by the  $\phi$  mesons and their decay. In the further analysis we hope to understand this contribution and be able to make conclusions on in-medium modifications of  $K^+$  and  $K^-$  from the ratios of momentum distributions.

#### References

- [1] C. Fuchs, Prog. Part. Nucl. Phys. **56**, 1 (2006).
- [2] B. Hong *et al.*, Phys. Rev. C **57**, 244 (1998).
- [3] D.B. Kaplan and A.E. Nelson, Phys. Lett. B **175**, 57 (1986); G.E. Brown and M. Rho, Phys. Rev. Lett. **66**, (1991) 2720; G.Q. Li and C.M. Ko, Phys. Lett. B **338**, (1994) 118; M. Lutz, Phys. Lett. B **426**, 12 (1998); Nucl. Phys. A **574**, 755 (1994); T. Waas, N. Kaiser and W. Weise, Phys. Lett. B **379**, 34 (1996); **365**, 12 (1996).
- [4] A. Gobbi *et al.* Nucl. Instr. Meth. A **324**, 156 (1993); J. Ritman *et al.*, Nucl. Phys. B, Proc., Suppl. **44**, 708 (1995).
- [5] N. Herrmann *et al.*, Ann. Rev. Nucl. Part. Sci. **49**, 581 (1999); W. Reisdorf and H.G. Ritter *et al.*, Ann. Rev. Nucl. Part. Sci. **47**, 663 (1997).
- [6] S. Voloshin and Y. Zhang, Z. Phys. C **70**, 665 (1996).
- [7] P. Danielewicz, G. Odyniec, Phys. Lett. **157B**, 146 (1985).
- [8] Jean-Yves Ollitrault, Nucl. Phys. A **638**, 195c (1998).

- [9] V. Zinyuk *et al.*, arXiv:1403.1504v2.
- [10] A. Andronic *et al.*, Phys. Lett. B **612**, 173 (2005).
- [11] P. Crochet *et al.*, Phys. Lett. B **486**, 6 (2000).
- [12] W. Cassing *et al.*, Phys. Rep. **308**, 65 (1999) .
- [13] C. Hartnack *et al.*, Eur. Phys. J. A **1**, 151 (1998).
- [14] W. Cassing *et al.*, Nucl. Phys. A **727**, 59 (2003).
- [15] C. Hartnack *et al.*, Phys.Rep. **510**, 119 (2012).
- [16] G.Q. Li and G.E. Brown, Nucl. Phys. A **636**, 487 (1998).
- [17] V. Zinyuk *et al.*, PoS Bormio2013 (2013) 066.
- [18] M.L. Benabderrahmane *et al.*, Phys. Rev. Lett. **102**, 182501 (2009).
- [19] M. Bueschner *et al.*, Eur. Phys. J. A **22**, 301 (2004).